Fluorescent Choleretic and Cholestatic Bile Salts Take Different Paths across the Hepatocyte: Transcytosis of Glycolithocholate Leads to an Extensive Redistribution of Annexin II

Joanne C. Wilton, Glenn M. Matthews, Robert D. Burgoyne,* Charles O. Mills, J. Kevin Chipman, and Roger Coleman

School of Biochemistry, The University of Birmingham, Edgbaston, Birmingham B15 2TT; and *The Physiological Laboratory, The University of Liverpool, Liverpool L69 3BX, United Kingdom

Abstract. We have used fluorescent derivatives of the choleretic bile salts cholate and chenodeoxycholate, the cholestatic salt lithocholate, and the therapeutic agent ursodeoxycholate to visualize distinct routes of transport across the hepatocyte and delivery to the canalicular vacuole of isolated hepatocyte couplets.

The cholate and chenodeoxycholate derivatives produced homogeneous intracellular fluorescence and were rapidly transported to the vacuole, while the lithocholate analogue accumulated more slowly in the canalicular vacuole and gave rise to punctate fluorescence within the cell. Fluorescent ursodeoxycholate showed punctate intracellular fluorescence against a high uniform background indicating use of both pathways.

Inhibition of vesicular transport by treatment with colchicine and Brefeldin A had no effect on the uptake of any of the compounds used, but it dramatically impaired delivery of both the lithocholate and the ursodeoxycholate derivatives to the canalicular vacuole.

We conclude that while the chenodeoxycholate and cholate analogues traverse the hepatocyte by a cytoplasmic route, lithocholate and ursodeoxycholate analogues are transported by vesicle-mediated transcytosis.

Treatment of couplets with glycine derivatives of lithocholate and ursodeoxycholate, but not cholate or chenodeoxycholate, led to a marked relocalization of annexin II, which initially became concentrated at the basolateral membrane, then moved to a perinuclear distribution and finally to the apical membrane as the incubation progressed. This suggests that lithocholate and ursodeoxycholate treatment leads to a rapid induction of transcytosis, and that annexin II exchange occurs upon membrane fusion at all stages of the hepatocyte transcytotic pathway.

These results indicate that isolated hepatocyte couplets may provide an inducible model system for the study of vesicle-mediated transcytosis.

BILE formation and secretion are exclusive to the liver, and they are essential to the emulsification and digestion of fats in the small intestine and in the detoxication and excretion of potentially toxic endobiotic and xenobiotic substances. The primary force for bile formation is thought to be the hepatobiliary transport of osmotically active bile salts. The vast majority of bile salts (90%) are reabsorbed across the intestine and taken up by hepatocytes from the portal blood for reexcretion (Coleman, 1987), while the remainder are synthesized de novo in the hepatocytes. The uptake and reexcretion of bile salts involves three distinct processes: uptake across the sinusoidal (basolateral) membrane, intracellular movement, and finally secretion across the canalicular (apical) membrane. These processes may be performed by dedicated cytoplasmic transport systems or by vesicle-mediated transcytosis, but the relative contributions of each of these are yet to be determined and may vary according to the physiological state of the animal.

Three possible transporters for monomeric bile salts have been shown to be localized to the basolateral membranes of hepatocytes. One is a 48–49-kD protein, which is sodium dependent and multisubstrate specific with a K_m for uptake of taurocholate of 10–20 μM (Frimmer and Ziegler, 1988; Zimmerli et al., 1989), the second is a sodium-independent multispecific anion carrier of 54 kD (Hugentobler and Meier, 1986), and a third electrogenic sodium-bile salt cotransport system has recently been described (Weinman and Weeks, 1993). A number of cytosolic proteins have been

implicated in carrier-mediated transport of bile salts across the cell. The 3α-hydroxysteroid dehydrogenases are probably the primary bile acid carriers in rats, although glutathione transferase and, to a far lesser extent, fatty acid-binding proteins may also perform this function (Stolz et al., 1989).

Excretion across the apical membrane into the bile canaliculus against a concentration gradient of 1:100 is the rate-limiting step in the movement of bile salts from the circulation (Meier, 1989), and it is the stage most susceptible to disruption in disease states. A 110-kD ATP-dependent glycoprotein has been identified as the primary bile salt transporter in the apical membrane (Nishida et al., 1991; Muller et al., 1991; Stieger et al., 1992). A 100-kD electrogenic bile acid transporting protein (Ruetz et al., 1987; Weinman et al., 1989) was thought to play a minor role in bile acid transport across the canalicular membrane, but recent evidence (Kast et al., 1994) has shown it to be restricted to the endoplasmic reticulum, where it has been suggested to participate in the modulation of the intracellular bile acid concentration.

In contrast to the situation in other polarized epithelial cells, newly synthesized hepatic membrane proteins are thought to move from the trans-Golgi network to the sinusoidal membrane, whereupon those destined for the apical pole undergo transcytosis to the canalicular membrane (Hubbard, 1991). This process depends on the integrity of a highly organized cytoskeleton. Under basal conditions, fluid phase endocytosis through this pathway contributes up to 10% of total bile flow (Lake et al., 1985; Sakisaka et al., 1988), but this largely comprises proteins and inert anions. Depolymerization of microtubules by colchicine treatment, however, delays the excretion of a high bile salt load delivered to perfused liver (Crawford et al., 1988), indicating a role for vesicle-mediated transcytosis in bile salt excretion in the postabsorptive state, when near-micellar concentrations of bile salts are reached in the portal vein.

Hepatocytes are not a homogeneous population. Numerous studies have demonstrated that opposing transport mechanisms and metabolic pathways are situated in different zones of the liver (reviewed by Jungermann and Katz, 1989) and have led to the concept of zonation of a variety of hepatic functions along the liver acinus. Although all hepatocytes are capable of extracting bile salts from the portal blood, there is an acinar gradient with the periportal cells (those most proximal to the portal vein) taking up the majority of the portal load (Groothuis et al., 1982), while the perivenous cells (those most distal) are largely responsible for bile salt synthesis. The possibility that different bile salt transport mechanisms are used by hepatocytes from distinct zones of the liver is appealing, with high capacity uptake in the periportal zone and high affinity uptake in the perivenous region to ensure minimal release of bile salts into the systemic circulation. This is certainly true of hepatic ammonia uptake (Haussinger, 1990).

Hepatocyte couplets, in which the polarity of hepatocytes is maintained, provide a model for the investigation of bile salt uptake and transport (Boyer, 1993), and can be separated into periportal- and perivenous-enriched fractions (Wilton et al., 1993a). Furthermore, these are primary cells, so they have a number of advantages over cultured cell lines in terms of morphology, enzyme activity, and distribution, and they

do not rely on long-term culture conditions for the development of polarized function. In this paper, we describe the use of a series of novel fluorescent bile salt derivatives (Mills et al., 1991) to visualize the transport of bile salts across the hepatocyte and the canalicular membrane. The bile salt derivatives selected behave as the glycine conjugates of the choleretic (bile flow–inducing) bile salt cholate and chenodeoxycholate, the cholestatic (bile flow–restricting) lithocholate, and ursodeoxycholate (a bile acid characteristic of bears), which is used clinically to restore biliary function in pathophysiological states, where it has been shown to be a potent anticholestatic agent via a number of ill-defined mechanisms. Secondly, the effects of colchicine and of Brefeldin A (BFA),[1] which inhibits transcytosis in polarized cells (Hunziker et al., 1991), upon the movement of these fluorescent bile salt derivatives, are demonstrated. Finally, we give evidence that these effects correspond with the redistribution of annexin II, a protein that participates in a number of membrane fusion events.

Materials and Methods

Materials

The fluorescent bile salts chenodeoxycholyl-lysyl-fluorescein (CDCLF), cholyl-lysyl-fluorescein (CLF), lithocholyl-lysyl-fluorescein (LF), and ursodeoxycholyl-lysyl-fluorescein (UF) were purchased from Dr. C. O. Mills (Liver Research Laboratories, Queen Elizabeth Hospital, Edgbaston, Birmingham, U.K.), all with purity >98%. Type A collagenase was obtained from Boehringer Mannheim (Lewes, East Sussex, U.K.). Sodium pentobarbital (Sagatal) was obtained from Animal Health Ltd. (Dagenham, Essex, U.K.). Leibowitz 15 (L-15) tissue culture medium supplemented with 2 mM glutamine was obtained from Gibco (Paisley, Scotland, U.K.). BSA (fraction V) was purchased from Winlab (Maidenhead, Berks, U.K.). Triton X-100, normal rat serum, normal rabbit serum, biotinylated goat anti-rabbit Ig G, FITC-labeled phalloidin, and colchicine were all purchased from Sigma (Poole, Dorset, U.K.). Glycochenodeoxycholic acid, glycocholic acid, glycolithocholic acid, and glycoursodeoxycholic acid were from Calbiochem-Novabiochem Ltd. (Nottingham, U.K.). Streptavidin Texas red was from Amersham International (Aylesbury, Bucks., U.K.). Diazabicyclo[2,2,2]octane was purchased from Aldrich Chemical Co. (Gillingham, Dorset, U.K.). Preparation of the anti-annexin II was described by Handel et al. (1991). Brefeldin A was from Epicentre Technologies (Cambio, Cambridge, U.K.). All other fine-grade chemicals were obtained from Sigma or British Drug Houses (Poole, Dorset, U.K.).

Animals

Male Wistar rats (230–250 g) were allowed free access to food (Standard Laboratories Ltd., Betchworth, Surrey, U.K.) and water before surgery, which was performed between 0800 and 0900 h. All the rats were housed in an environment with constant temperature and humidity, and alternating 12-h light and dark cycles.

Isolation of Hepatocyte Couplets

Rat hepatocyte couplets were isolated using a modification (Wilton et al., 1993b) of the methods described by Phillips et al. (1982) and Gautam et al. (1987). Centrifugal elutriation was used to generate two couplet-enriched preparations of predominantly periportal and perivenous origin (Wilton et al., 1993a). This was performed using a JE-5.0 rotor head mounted on a JE6-B centrifuge (Beckman Instruments, High Wycombe, Bucks, U.K.). The rotor and elutriation buffer (Krebs-Henseleit solution containing 1% (wt/vol) glucose and BSA, pH 7.4) were maintained at room

temperature (21°C). The rotor speed was maintained at 850 rpm throughout the separation process. Cells were loaded into the separation chamber at a buffer flow rate of 10 ml/min, and the nominated periportal- and perivenous-enriched fractions were collected at flow rates of 28–31 and 40–43 ml/min, respectively. This combination of rotor speed and collection flow rates had been shown to separate periportal and perivenous couplets without causing cell damage. During collection, fractions were kept on ice, then centrifuged at 500 rpm for 5 min. The cell pellets were resuspended in L-15 medium (4 ml), and the population of couplets in each fraction were counted using a Neubauer hemocytometer (British Drug Houses, Poole, Dorset, U.K.). Viability was determined by assessment of Trypan blue exclusion (Moldeus et al., 1978).

Elutriation removed most of the dead or damaged cells present in suspensions of mixed hepatocyte populations. The viability of the periportal and perivenous couplets at plating was therefore high at 97.6 ± 1.2% (mean ± SEM) and 98.5 ± 0.9%, respectively. The proportion of couplets in the elutriated preparations was >78% in the periportal fraction (where the major contaminant was single cells) and >82% in the perivenous fractions (where the contaminants were hepatocyte triplets).

Culture of Hepatocyte Couplets

Cells used in the assessment of uptake of fluorescent bile salts and of canalicular activity were plated in 35-mm diameter tissue culture dishes (CelCult; Sterilin, Harlow, Essex, U.K.) at 1×10^5 couplets/plate in 2 ml of L-15 medium. Cells used for localization of f-actin and for immunocytochemical staining of annexin II were added to plates containing 10-mm diameter glass coverslips. All cells were incubated for 5.5 h (to include treatment period, see below) at 37°C.

Canalicular vacuoles were visualized after incubation with the fluorescent cholephiles CDCLF, CLF, LCLF, and UCLF. The appropriate stock solution (2 µl; 2 mM CDCLF, CLF, LCLF, and UCLF in 0.9% [wt/vol] NaCl) was added to the sample dishes and incubated at 37°C for 5, 10, 15, 30, 45, or 60 min. The couplets were washed with L-15 medium (37°C) twice before examination with an inverted fluorescence microscope (IM2-RFL; Olympus Corp., Precision Instruments Division, Lake Success, NY) with a stage incubator. Monochrome images of the couplets were recorded (KP-116 camera; Hitachi Instruments, Inc., San Jose, CA) and contrast enhanced (CE-2 contrast enhancer; Brian Reece Scientific, Newbury, Berks, U.K.). The length and area of the couplets and their canalicular vacuoles were determined using an image analysis system (Mini-Magiscan; Applied Imaging, Sunderland, U.K.).

The development of canalicular secretory activity was assessed in randomly chosen fields of view. All the couplets in a designated field were counted ($n > 50$). Couplets exhibiting active canalicular secretion of a fluorescent bile salt into a sealed canalicular vacuole were measured as a proportion of the total number of couplets present.

Uptake of Fluorescent Bile Salts

Mixed (population-matched) cultures of periportal and perivenous couplets were incubated with CDCLF, CLF, LCLF, or UCLF as described above for up to 60 min. The cultures were washed twice with 2.0 ml of PBS, pH 7.4. The cells were then scraped off the culture plates in 4.0 ml distilled water (2 × 2.0 ml) and sonicated for 3 × 6 s (Dawe sonicator; Lucas Dawe Instruments, Middlesex, U.K.). Cell debris was removed by centrifugation at 1300 rpm for 2 min. The fluorescence present in the sonicate was determined using a luminescence spectrometer (LS 50B; Perkin Elmer, High Wycombe, Bucks., U.K.) using an excitatory wavelength of 495 nm and an emission wavelength of 525 nm, which was calibrated using standard solutions of fluorescent bile salts. Total fluorescent bile acid content of the cells was expressed in terms of picomoles of fluorescent bile salt per 10^6 cells.

Incubation with Colchicine and Brefeldin A

Couplets were plated as described above and 1 h before the addition of the fluorescent bile salt derivatives, colchicine was added to the culture medium to a final concentration of 60 nM (from a stock solution of 60 µM colchicine in physiological saline). In a separate experiment, hepatocyte couplets were incubated with 10 µM BFA (stock of 5 mg/ml in ethanol) for 15 min before the addition of the fluorescent bile salt derivatives. These treatments, which are milder than those used in other studies (Sakisaka et al., 1988; Hunziker et al., 1991), were optimized to ensure that the minimum active concentration of each reagent was used, thereby reducing the likelihood that the effects were caused by nonspecific cell damage.

Fluorescent Staining of Actin

Periportal and perivenous couplet preparations seeded onto glass coverslips were incubated for a total incubation period of 5.5 h that included incubation with 2.0 µM glycine conjugates of chenodeoxycholate (GCDC), glycocholate (GC), lithocholate (GLC), or ursodeoxycholate (GUDC) for 0, 15, 30, 45, or 60 min before fixation in 3% (wt/vol) formaldehyde in PBS. Stock 2-mM solutions of the bile salts were made up in saline. The cells were labeled using a modification of the method described by Knutton et al. (1989). Briefly, PBS washed cells were permeabilized by soaking the coverslips in 0.1% (vol/vol) Triton X-100 in PBS for 4.0 min. After washing in PBS, the cells were treated with FITC-phalloidin (5 µg/ml in PBS) for 20 min to specifically label filamentous actin (Clerc and Sansonetti, 1987). The cells were washed again in PBS before mounting in 90% glycerol-PBS containing 2.5% (wt/vol) diazabicyclo[2,2,2]octane. The specimens were examined under fluorescent light (excitation wavelength 490 nm, emission wavelength >525 nm) using an inverted Zeiss microscope (Axiovert 350TV; Carl Zeiss Oberkochen Ltd., Welwyn Garden City, Herts, U.K.) equipped with Zeiss plan-neofluar lenses. Monochrome images taken in 1.0-µm steps (Prior, Cambridge, U.K.) were captured on a CCD video camera (Hamamatsu Photonic Sys. Corp., Hamamatsu City, Japan) and out-of-focus-flair removed using a deconvolution program (Micro-Tome Mac, Vaytek Ltd., Fairfield, IL). Images were analyzed using the Fluovision program (Improvision, Warwick Science Park, Coventry, U.K.).

Fluorescent Staining of Annexin II

Localization of annexin II was based on the method described by Handel et al. (1991). Formaldehye-fixed couplets on coverslips (see above) were washed three times with PBS, then treated with a permeabilized buffer (0.1% Triton X-100 in PBS containing 0.3% [wt/vol] BSA) for 7 min before a PBS wash and incubation with normal rat serum (1:50) for 6 h at room temperature. The cells were washed three times in the permeabilization buffer before incubation at 4°C for 18 h with anti-annexin II antiserum (1:800). Cells were again washed three times in permeabilized buffer before a 1-h incubation with biotinylated anti-rabbit antibody (1:100) followed (after washing) by streptavidin–Texas red (1:100). Nonimmune rabbit serum was used instead of the anti-annexin II antibody on samples subjected to all treatments as a negative control. After a final wash in PBS, the cells were mounted and examined by fluorescence microscopy with image analysis as described for actin, except that excitation was at a wavelength of 540 nm, and emission was >580 nm. The specificity of the antibody against hepatocyte proteins was verified by Western blotting.
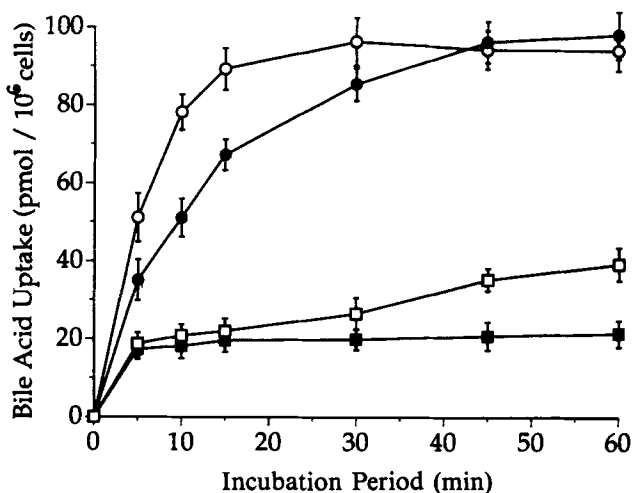

Figure 1. Total content of fluorescent bile salt derivatives in primary cultures of hepatocyte couplets after incubation for up to 60 min with 2 µM CDCLF (–○–), CLF (–●–), UCLF (–□–) or LF (–■–). Fluorescence was determined as described in Materials and Methods. Content is expressed in terms of picomoles of fluorescent bile salt per 10^6 cells, and values are expressed as means ± SEM ($n = 6$).

Table I. Qualitative Assessment of Cytoplasmic and Canalicular Uptake of the Fluorescent Cholephiles CDCLF, CLF, LCLF, and UCLF after 5, 15 and 45 min of Incubation at 37°C

Bile salt	Time	Cytoplasmic uptake	Canalicular uptake	Comments
CDCLF	5	+	+ + + +	Homogeneous
	15	+ +	+ + + + +	Homogeneous
	45	+ +	+ + + + +	Homogeneous
CLF	5	+	+ + + +	Homogeneous
	15	+	+ + + + +	Homogeneous
	45	+	+ + + + +	Homogeneous
LF	5	ND	ND	
	15	+ +	+ + +	Punctate
	45	+ + +	+ + + +	Punctate
UF	5	+	+ + +	Homogeneous
	15	+	+ + + +	Punctate
	45	+ +	+ + + +	Punctate

The arbitrary scale runs from + (visible) to + + + + + (very intense fluorescence). ND, inability to detect by eye any fluorescence. The comments refer to the cytoplasmic uptake of the bile salts.

Results

Uptake of Fluorescent Bile Salt Derivatives

The total uptake of the fluorescent bile salt derivatives by hepatocyte couplets over time is shown in Fig. 1. These values include both the fluorescence present within the cells and that which is secreted into the canalicular vacuole that forms between them. CDCLF and CLF accumulated to approximately equivalent steady-state levels, although this was reached more rapidly by CDCLF. LCLF and UCLF were taken up less efficiently, reaching 20% and 38%, respec-

tively, of the CDCLF/CLF level after 60 min. The level of UCLF uptake continued to increase during the incubation period, in contrast to LCLF, which remained constant after the first 30 min.

These results were reflected by the appearance of the cultures (Table I, Fig. 2). Couplets incubated with CDCLF and CLF displayed highly fluorescent canalicular vacuoles, with a lower, homogeneous signal throughout the cytoplasm (Fig. 2, A and B). The difference in total uptake of these fluorescent bile salts at early time points (Fig. 1) resulted from higher cellular fluorescence in couplets incubated with CDCLF. This may reflect a more rapid sinusoidal uptake of CDCLF that exceeds the capacity of the canalicular transport mechanism to excrete it into the vacuole.

At early time points the fluorescence in LCLF-treated couplets was restricted to the cytoplasm and had a marked "marbled" appearance (Fig. 2 D). As the incubation progressed, the extent of this marbling increased, and the signal moved into the vacuole with a prevalence of brightly fluorescent vesicles within the pericanalicular area, particularly of perivenous couplets. At early and intermediate stages of the LCLF treatment (15–30 min), punctate canalicular labeling could be seen surrounding the unlabeled but enlarged vacuole in some couplets (Fig. 3).

The uptake characteristics of UCLF were intermediate between those of CDCLF/CLF and of LCLF, showing both homogeneous cytoplasmic fluorescence and punctate signal (Fig. 2 C). The vacuoles of these couplets were better defined than those of LCLF-treated couplets.

Canalicular Accumulation of Fluorescent Bile Salt Derivatives

Previous work from this laboratory (Wilton et al., 1993a) has shown that after 5.5 h of culture at 37°C, >80% of
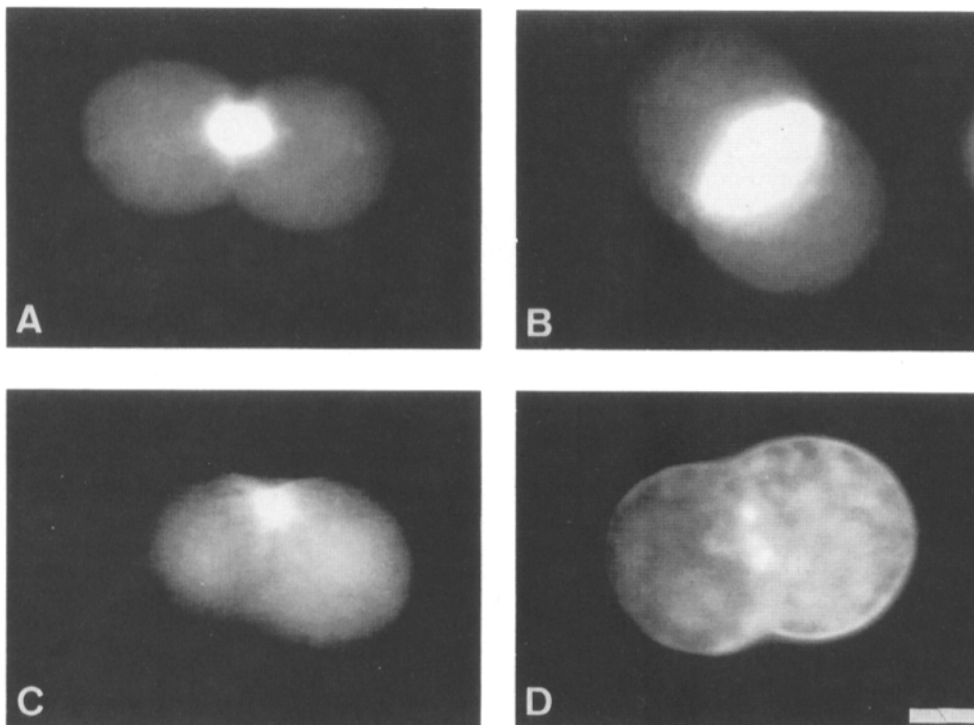

Figure 2. Visualization of bile acid uptake using fluorescent bile salt derivatives. Couplets were incubated in 2 μM CDCLF (A), CLF (B), UCLF (C), or LCLF (D) for 15 min before washing and visualization using fluorescence microscopy (see Materials and Methods for details). Bar, 10 μm.
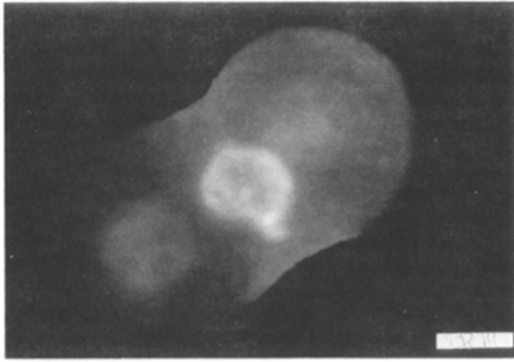
Figure 3. Approximately 30% of perivenous couplets incubated with 2 μM LCLF for 30 min exhibit highly labeled canalicular membranes surrounding an open but unlabeled canalicular vacuole. Bar, 10 μm.
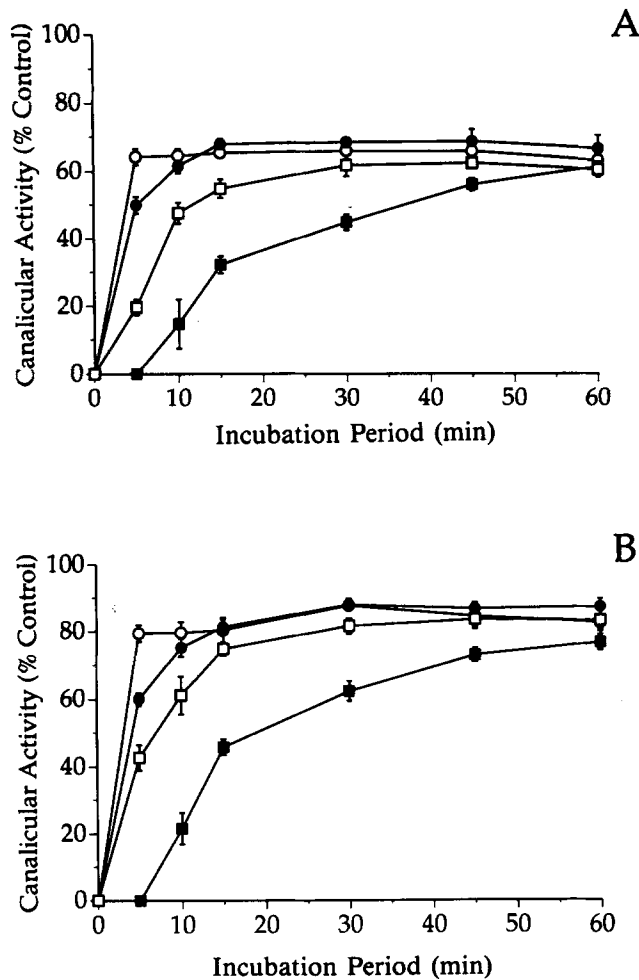
perivenous couplets and >60% of periportal couplets exhibit canalicular accumulation of CLF after a 15-min incubation. The time taken to reach these plateau levels varied for the other agents studied: CDCLF (5 min), UCLF (30 min), and LCLF (60 min) (Fig. 4, *A* and *B*). The development of visible fluorescent canalicular vacuoles was not discernible after 5 min of incubation with LCLF, and only barely so after 10 min. Only after 60 min did the intensity of the label in the canalicular vacuole of these couplets approach the levels seen with the other fluorescent bile salts at earlier time points.

Cellular and canalicular areas were determined by analysis of images captured during the estimation of canalicular accumulation. Table II shows changes in the area of the canalicular vacuole during the incubation period with each of the four fluorescent bile salt derivatives in periportal and perivenous hepatocyte couplets. Canalicular accumulation is a cyclic process, with vacuoles expanding as biliary components are secreted across the canalicular membrane, before contracting or collapsing and expelling their contents via a temporary rupture of the tight junctions between the adjacent cells. Each time point is therefore a "snap shot" of a mixture of enlarging and static vacuoles. The results shown in Table II clearly demonstrate that the canalicular vacuoles of periportal couplets are proportionally larger than those of perivenous couplets after treatment with CDCLF and CLF, but are equivalent after incubation with LCLF or UCLF. Some obvious differences were also observed between the various bile salts. In both periportal and perivenous couplets, canalicular vacuoles were larger in the presence of CLF than with any of the other bile salt derivatives. After prolonged incubation with CDCLF, vacuolar size was reduced; with CLF and UCLF, it was generally unchanged,

Figure 4. Development of canalicular secretory activity in periportal (*A*) and perivenous (*B*) hepatocyte couplets incubated with CDCLF (–o–), CLF (–●–), LCLF (–■–), or UCLF (–□–). Canalicular secretory activity was assessed as described in Materials and Methods. Each value is the mean ± SEM (*n* = 4 separate hepatocyte preparations, >50 couplets were assessed at each time point).

Table II. The Canalicular Vacuole Area/Total Cell Area Ratio in Periportal and Perivenous Hepatocyte Couplets Incubated with 2 μm CDCLF, CLF, LCLF, or UCLF for 15, 30, 45, or 60 min

Time	Zone	CDCLF	CLF	LF	UF
mins					
15	pp	7.29	7.59	3.12	4.52
		0.32	0.59	0.64	0.55
15	pv	4.03	5.79	2.33	3.48
		0.36	0.57	0.53	0.81
30	pp	6.72	7.42	3.57	4.96
		0.74	0.61	0.55	0.60
30	pv	4.42	5.48	2.51	4.65
		0.48	0.48	0.38	0.59
45	pp	4.72	7.56	4.82	4.55
		0.47	0.74	0.57	0.59
45	pv	3.64	5.52	4.62	4.61
		0.34	0.65	0.79	0.54
60	pp	4.69	7.52	6.43	4.56
		0.39	0.73	0.74	0.62
	pv	3.75	5.63	6.24	4.51
		0.32	0.72	0.48	0.34

Figures represent the mean ± SEM of 20 couplets taken from four rats. pp, periportal; pv, perivenous.
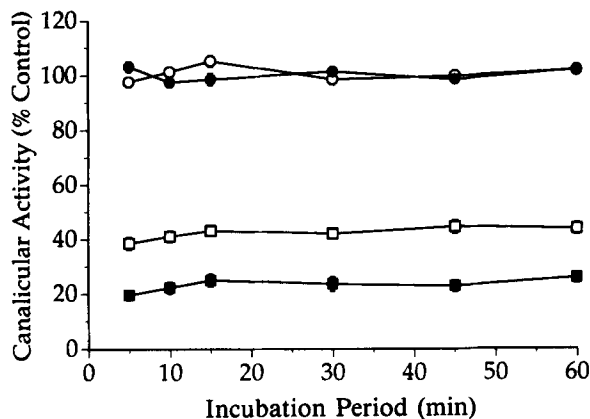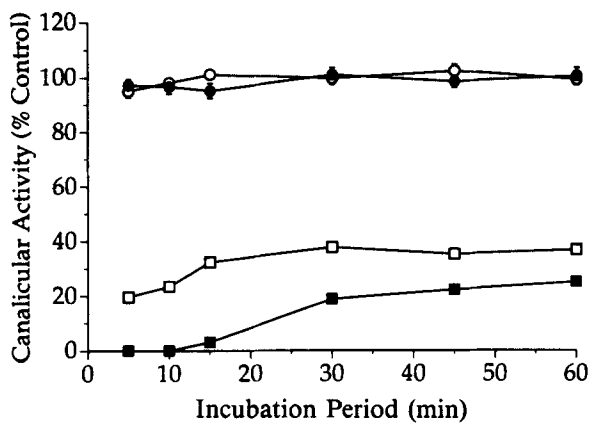
A

B

Figure 5. The effect of colchicine on canalicular secretory activity in periportal (A) and perivenous (B) hepatocyte couplets incubated with fluorescent bile salt derivatives for up to 60 min. Couplets were incubated with 60 nM colchicine for 60 min before addition of CDCLF (–o–), CLF (–●–), LCLF (–■–), or UCLF (–□–) for 0–60 min (see Materials and Methods for details). Canalicular secretory activity is expressed as the percent control value at each time point and for each fluorescent cholephile. Each value is the mean ± SEM (n = 4 separate hepatocyte preparations, >50 couplets were assessed at each time point).

but with LCLF there was a steady increase in vacuolar area with time.

The Effect of Transport Inhibitors

To examine the role of microtubules in the development of canalicular vacuoles, couplets were preincubated with 60 nM colchicine for 60 min before incubation with bile salt derivatives. These experiments (summarized in Fig. 5 and Table III) demonstrated that colchicine had no effect on the numbers of couplets accumulating CDCLF or CLF in their canalicular vacuoles at any time point, but it caused a marked reduction in the number accumulating UCLF and, to a greater extent, LCLF, which were reduced to 25% of control levels. Preincubation with colchicine caused a reduction in vacuolar size, irrespective of the bile salt used, in periportal couplets assessed after a 15-min incubation (Table III), as well as in perivenous couplets treated with LCLF and UCLF. The relative areas recovered to control levels within

A

Table III. The Percentage of Control Values of the Proportion of the Canalicular Area to Couplet Area of Periportal and Perivenous Hepatocyte Couplets Incubated with 2 μM CDCLF, CLF, LCLF, or UCLF for 15, 30, 45, or 60 min after a 1-h Preincubation with 60 nM Colchicine

Time	Zone	CDCLF	CLF	LF	UF
15	pp	56.4	43.6‡	0	38.7‡
		12.3	9.1		15.0
15	pv	92.1	73.2	37.3‡	44.0‡
		7.1	7.1	11.9	5.9
30	pp	63.1	42.0‡	12.3‡	49.6
		8.9	15.9	22.5	12.3
30	pv	85.7	97.4	36.3‡	35.3‡
		11.4	11.1	10.0	7.7
45	pp	97.7	91.3	43.6‡	107.2
		10.2	10.6	5.6	11.7
45	pv	101.1	90.7	30.5‡	88.1
		10.1	10.1	7.9	14.9
60	pp	93.6	90.7	57.6*	103.5
		7.1	8.4	10.8	11.4
60	pv	104.3	96.3	34.5‡	101.1
		10.3	10.4	4.2	9.4

Figures represent the mean ± SEM of 20 couplets taken from four rats. The superscripts relate to significant differences between colchicine-treated and control values. *$P < 0.05$, ‡$P < 0.01$.

45 min in all but LCLF-treated cells, which remained much smaller at 58% of control values for periportal couplets and only 34.5% in the perivenous preparation after 60 min. Pretreatment with colchicine did not inhibit the initial step in vesicular uptake of LCLF or UCLF, as the accumulation of fluorescently labeled vesicles adjacent to the plasma membrane of these cells demonstrates. Rather, the effect was on transport to the canalicular membrane.

Preincubation with 10 μM BFA for 15 min dramatically reduced subsequent canalicular accumulation of both LCLF and UCLF in hepatocyte couplets (Fig. 6) at all the time points examined. Little change in accumulation was noticed with CDCLF and CLF, but with UCLF accumulation, it was reduced to 23% of control levels in perivenous hepatocytes and a little more than 10% of control values in periportal couplets. LCLF accumulation was completely absent in periportal couplets after pretreatment with BFA, and it was reduced to <10% of control values in perivenous cells.

Fluorescent Staining of F-Actin

The characteristic staining pattern for F-actin in hepatocyte couplets (Fig. 7 A) was unchanged by incubation of couplets with 2 μM GC, GCDC, GLC, or GUDC for up to 60 min (data not shown). Preincubation with 60 nM colchicine for 60 min did not significantly alter F-actin distribution in control or in bile salt-treated couplets (Fig. 7 B).

Fluorescent Staining of Annexin II

In control couplets of both periportal and perivenous hepatocytes, detection of annexin II by indirect immunofluorescence gave a sparse homogeneous signal with no marked delineation of the plasma membrane and no signal in the
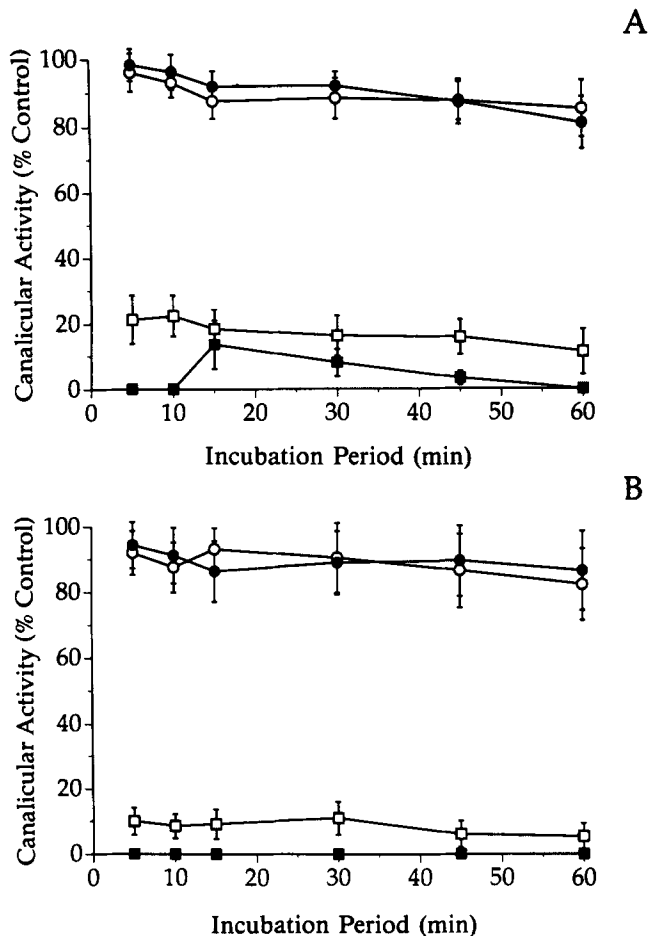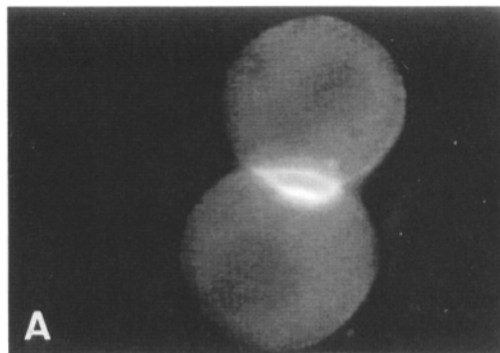
A

B

Figure 6. The effect of Brefeldin A on canalicular secretory activity in periportal (*A*) and perivenous (*B*) hepatocyte couplets incubated with fluorescent bile salt derivatives for up to 60 min. Couplets were incubated with 10 μM BFA for 15 min before addition of CDCLF (–○–), CLF (–●–), LCLF (–■–), or UCLF (–□–) for 0–60 min (see Materials and Methods for details). Canalicular secretory activity is expressed as the percent control values at each time point and for each fluorescent cholephile. Each value is the mean ± SEM (*n* = 4 separate hepatocyte preparations, >50 couplets were assessed at each time point).

Figure 7. Accumulation of actin at the apical pole of hepatocyte couplets. Preincubation of the couplets for 60 min with 60 nM colchicine (*A*) did not effect pericanalicular staining relative to control (*B*) treatment. Bar, 10 μm.

pericanalicular region (Fig. 8 *A*). This pattern changed markedly upon incubation with 2 μM GLC or GUDC.

After 15 min of incubation (Fig. 8 *B*), the majority of the annexin II staining was immediately beneath the basolateral membrane with a gradient toward the perinuclear region of the cells, although it was notably absent from the nuclear region itself. After 30 min (Fig. 8 *C*), the signal had become more concentrated with clear perinuclear staining and more intense fluorescence from the perinuclear area toward the canalicular membrane, which was also labeled, although at a relatively low intensity. Pericanalicular staining had become bright and punctate by 45 min (Fig. 8 *D*), when the perinuclear signal was tighter but still present. Annexin II was never present within the nucleus and, after 45 and 60 min of incubation with GLC or GUDC, the majority of the staining was in the pericanalicular area.

Examination of the staining pattern at earlier time points of GLC treatment (Fig. 9) showed that the accumulation of the localized signal is rapid. Couplets fixed only 1 min after the addition of GLC showed clear staining for annexin II
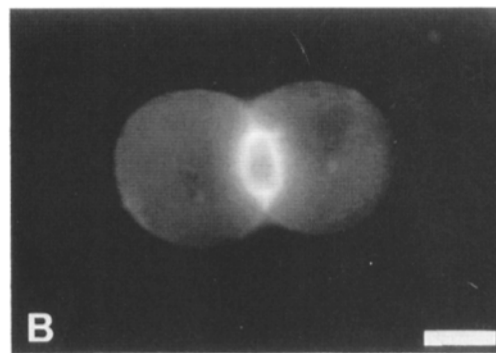
(Fig. 9 *A*), which became localized to patches on the inner surface of the plasma membrane after 2 min (Fig. 9 *B*). These patches extended and increased in intensity in samples fixed after 5 min of treatment (Fig. 9 *C*) to form a tight contiguous signal covering the inner face of the entire plasma membrane except for the canalicular pole.

Treatment with LCLF gave rise to a redistribution of annexin II identical to that seen with GLC (data not shown), while incubation with GCDC and GC showed some redistribution of annexin II staining, but to a far lesser extent than with GLC or GUDC.

Discussion

The data presented demonstrate qualitative and quantitative differences between the fluorescent bile salts used, which reflect different modes of uptake and transport across the hepatocyte. CDCLF and CLF are taken up efficiently and are rapidly excreted into the canalicular vacuole by a process that is insensitive to BFA and relatively unaffected by the colchicine regime used, especially in perivenous couplets. Conversely, cellular uptake of LCLF and its delivery to the vacuole is slow, has a relatively low capacity, and is sensitive to BFA and colchicine. UCLF appears to use a pathway that has characteristics of both of these, or to be transported by both routes. The patterns of intracellular fluorescence generated also vary, with CLF and CDCLF giving rise to a homogeneous signal, while LCLF and UCLF show a more punctate
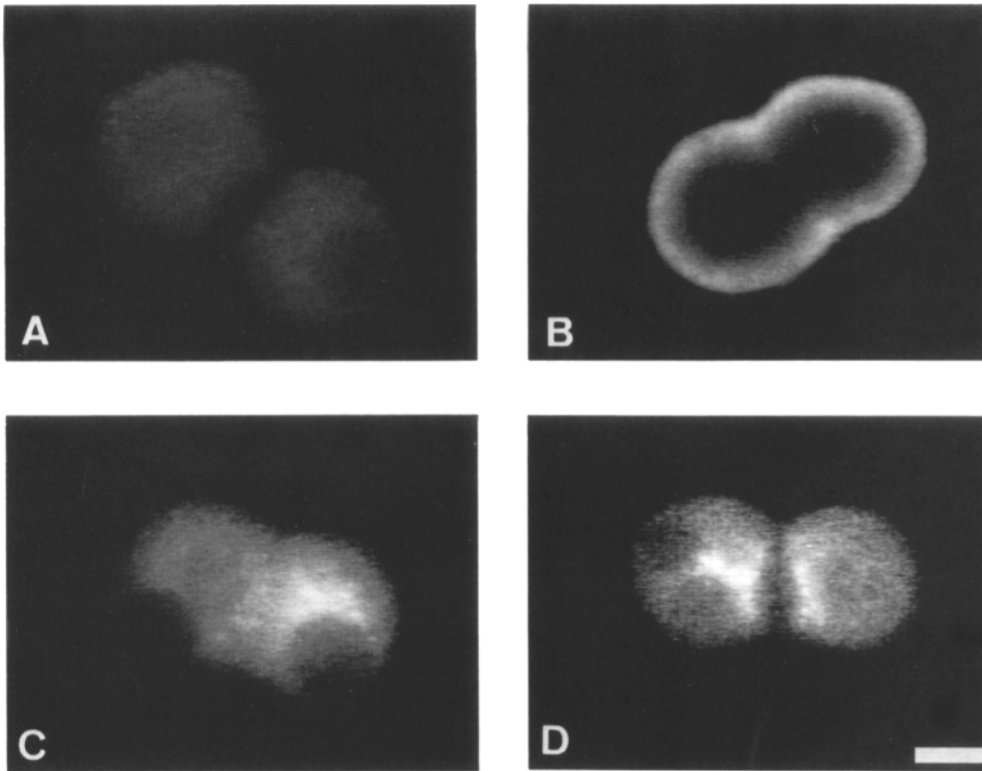
Figure 8. Redistribution of annexin II in couplets incubated with 2 μM glycolithocholate for 0 (*A*), 15 (*B*), 30 (*C*), and 45 (*D*) min. The signal is sparse and uniformly distributed throughout the cytoplasm in untreated cells (*A*). After treatment with GLC, the signal increases and becomes concentrated at the plasma membrane (*B*) and subsequently relocalizes to a perinuclear distribution (*C*) before accumulating at the canalicular membrane (*D*). Bar, 10 μm.

distribution. Treatment of hepatocyte couplets with lithocholate caused a redistribution of annexin II, indicating a significant stimulation of vesicle-mediated transport to the canalicular membrane.

The uniformity of intracellular fluorescence and the rate of transport across the cell indicate that CLF and CDCLF are taken up across the basolateral membrane, cross the cell by a cytoplasmic route, and are released specifically at the canaliculus. These fluorescent bile salt derivatives (FBSDs) probably use the bile acid transporters present as previously described in the basolateral (Zimmerli et al., 1989; Weinman and Weeks, 1993) and canalicular (Kast et al., 1994) membranes. The punctate pattern of intracellular fluorescence generated by LCLF and its slower delivery to the canalicular vacuole indicate that its route to the canalicular membrane involves at least a component of vesicle-mediated transport. It is not possible at present to distinguish between vesicular uptake via the endocytic pathway and uptake by plasma membrane transporters followed by a rapid secondary transport step from the cytoplasm into the endomembrane system. It is unlikely that the differences observed between the fluorescent bile salt derivatives used resulted from the presence of the lysyl-fluorescein moiety, because this is attached at the same position (C_{24}) in all cases, and the derivatives exhibit similar kinetics of biliary excretion in vivo as the glycine conjugates of the parent bile salts (Mills et al., 1991; Mills, C. O., personal communication). Certainly the uptake of CDCLF and CLF into hepatocyte couplets is reduced in a dose-dependent manner in the presence of their glycine conjugates (Wilton, J. C., unpublished data), which indicates that the same saturable mechanism is used regardless of the presence of the fluorescent moiety.

Comparison of the ratios of canalicular vacuole to cell area

in periportal and perivenous couplets (Table II) further demonstrates differential activity between the routes taken by the different bile salts. For CLF and CDCLF, the canalicular vacuoles produced were proportionally ~50% larger in periportal than in perivenous couplets while less, if any, difference is evident between the populations upon LCLF or UCLF treatment. Hepatic clearance of plasma bile acids is critical. In the liver, periportal hepatocytes are exposed to higher bile acid concentrations than perivenous hepatocytes, and it is possible that the larger canalicular vacuoles of periportal couplets exposed to CDCLF and CLF reflect a more efficient carrier-mediated transport mechanism of these FBSDs. Endocytotic uptake, transcytosis, and exocytosis of LCLF and UCLF, however, appear to be unaffected by lobular origin.

Inhibition of Transport

Colchicine blocks tubulin assembly, leading to the loss of directional vesicular transport, which relies on the presence of an intact microtubular network. Previous work using colchicine to inhibit vesicular movement in hepatocytes has used relatively high (10^{-5} M) concentrations of the inhibitor (Sakisaka et al., 1988). The treatment used in these experiments was very mild (60 nM) and had no effect on the integrity of the tight junctions between the couplets, as demonstrated by the canalicular accumulation of CDCLF and CLF, and little visible effect on the actin staining pattern. It did, however, dramatically reduce the rate of LCLF transport to the canalicular vacuole, particularly in perivenous couplets.

BFA acts by inhibiting guanine nucleotide exchange on ADP-ribosylation factor, the primary step in the formation of transport vesicles (Helms and Rothman, 1992; Donaldson et al., 1991), and it has been shown to inhibit transcytosis
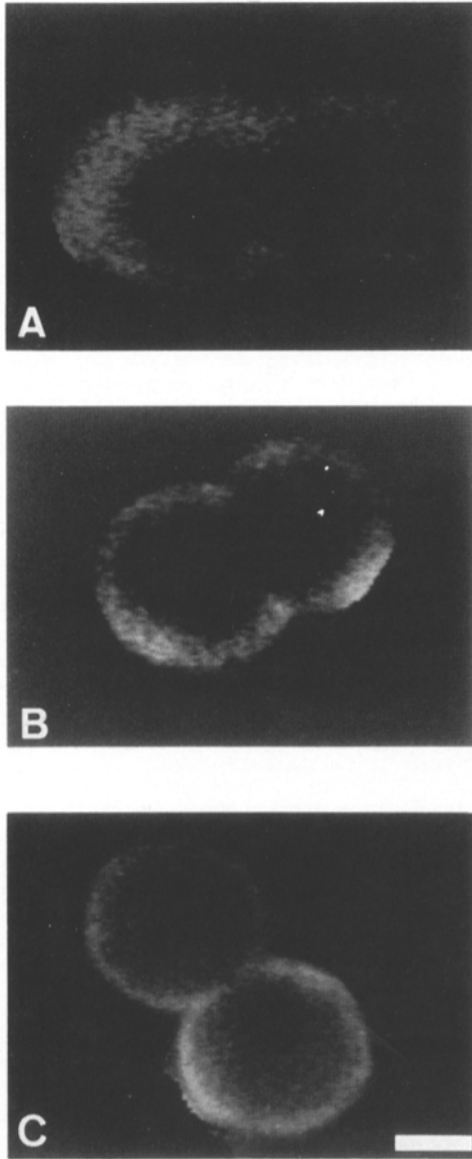
Figure 9. Early stages in the localization of annexin II to the basolateral membrane. Couplets were treated with GLC for 1 (*A*), 2 (*B*), and 5 (*C*) min before fixation and immunolocalization of annexin II. Within 1 min of treatment (*A*), the signal begins to concentrate and move to the membrane, where it becomes localized in patches (*B*) that spread to form a contiguous signal by 5 min of treatment (*C*). Bar, 10 μm.

in MDCK cells (Hunzicker et al., 1991). In this experiment, it had minimal effect on the transport of CDCLF and CLF, while it almost completely prevented LCLF transport.

In view of their completely distinct modes of action, the similarity between the effects of colchicine and BFA on LCLF delivery to the canalicular vacuole strongly indicates a role for vesicle-mediated transport in this process.

A simple explanation for the differences between the behavior of LCLF and CDCLF/CLF would be that LCLF is incapable of interacting with the basolateral transporter, and so its only available route across the cell is by fluid phase transcytosis, thus revealing this pathway, which may play only a minor role in the delivery of the choleretic bile salts

to the canaliculus. Preliminary data from experiments in which couplets were challenged with mixtures of GLC and CLF, as well as GC and LCLF (Wilton, J. C., unpublished data), indicate that while GC has no effect on LCLF uptake, GLC inhibits the uptake of CLF, probably at the level of the transporter, which corresponds with the known cholestatic activity of lithocholate. The failure of the couplets to accumulate CLF in the presence of GLC implies that fluid phase uptake cannot account for all the LCLF uptake observed. So far, experiments to establish whether LCLF uptake is receptor mediated have not been conclusive.

While periportal couplets appeared to be more sensitive to the effects of colchicine and BFA on vacuole formation and size, these differences are not sufficiently distinct to allow conclusions to be drawn on the relative importance of vesicle-mediated transport across the hepatic lobule.

Annexin II

Annexin II has been implicated in membrane fusion events leading to exocytosis (Sarafian et al., 1991; Drust and Creutz, 1988; Ali et al., 1989) and in the fusion and distribution of early endosomes (Emans et al., 1993; Harder and Gerke, 1993). The active membrane- and cytoskeleton-associated form of annexin II, calpactin 1, is a heterotetramer containing two subunits of each of annexin II and a second polypeptide, p11 (Gerke, 1991). The assembly of this complex may be controlled at the level of annexin II phosphorylation at sites for signal-transducing protein kinases in the NH$_2$-terminal 30 amino acid residues of annexin II. Protein kinase C–mediated phosphorylation, at Ser 25, is important for activity in calcium-regulated exocytosis (Sarafian et al., 1991), while Tyr 23 of annexin II is the major cellular target for phosphorylation by p60^{src}, which has been localized to endosomal membranes (Kaplan, 1992).

Treatment with GLC leads not only to a relocalization of annexin II, but also to an apparent increase in the amount of protein detected. This effect becomes apparent after 1 min and is complete by 15 min of exposure, and is therefore too rapid to be the result of new protein synthesis, but it is most likely to result from more efficient detection of the active heterotetramer. This may be caused by the loss of monomer upon permeabilization, the concentration of signal at sites of membrane/cytoskeletal attachment, the unmasking of an epitope upon recruitment into the active calpactin tetramer, or a combination of these effects. Whatever the reason, the increase in signal corresponds to a recruitment of annexin II into the active form and reflects a significant upregulation of membrane transport activity under these conditions. What mediates this effect is at present unclear, but it is tempting to speculate that specific signaling events may be involved.

The change in the pattern of annexin II distribution with time after GLC treatment implies that the initial uptake step effectively saturates the transcytotic capacity of the cell. The uptake of LCLF, at least, is abolished by preincubation with GLC (Wilton, J. C., unpublished data). This is followed by a wave of transport across the transcytotic pathway leading to delivery at the canalicular membrane. The time scale of the annexin II redistribution is similar to those associated with movement of HRP (Hayakawa et al., 1990), a marker for fluid phase transcytosis, and immunoglobulin A (Lowe et al., 1985), a marker for receptor-mediated transport, into

the bile of perfused rats, and to the canalicular membrane of isolated hepatocytes. Emans et al. (1993) demonstrated that annexin II is transferred upon fusion of early endosomes and reported its possible immunolocalization in BHK cells to endomembrane compartments other than early endosomal and exocytic vesicles. The perinuclear signal seen in the hepatocyte couplets at intermediate time points indicates at least transient relocalization of annexin II to the Golgi apparatus, and it implies that annexin II transfer occurs upon membrane fusion throughout the route taken by GLC to the canaliculus.

Studies of protein targeting in hepatocytes (Hubbard, 1991) have shown that newly synthesized apical membrane proteins are delivered first to the basolateral membrane, then selectively retrieved and transported to the apical membrane by transcytosis. This has been interpreted as indicating that there is no direct route from the Golgi apparatus to the apical membrane in these cells. This transcytotic pathway also appears to be the major fluid phase route across the cell (Barr and Hubbard, 1993). If lithocholate is transported via the Golgi apparatus, as implied indirectly by the intermediate perinuclear distribution of annexin II, this may constitute a second pathway across the hepatocyte, and future studies will address this issue.

The degree to which these events are induced upon lithocholate treatment indicates that isolated hepatocyte couplets may provide a useful model system where molecular events associated with the regulation of endocytosis and transcytosis can be studied.

References

Ali, S. M., M. Geisow, and R. D. Burgoyne. 1989. A role for calpactin in calcium-dependent exocytosis in adrenal chromaffin cells. *Nature (Lond.).* 340:313-315.

Barr, V. A., and A. L. Hubbard. 1993. Newly synthesised hepatocyte plasma membrane proteins are transported in transcytotic vesicles in the bile duct ligated rat. *Gastroenterology.* 105:554-571.

Boyer, J. L. 1993. Isolated rat hepatocyte couplets: a model for study of bile secretory function. *In* Hepatic Transport and Bile Secretion: Physiology and Pathophysiology. N. Tavoloni and P. D. Berk, editors. Raven Press, Ltd., New York. pp. 597-606.

Clerc, P., and P. J. Sansonetti. 1987. Entry of *Shigella flexneri* into HeLa cells: evidence for directed phagocytosis involving actin polymerization and myosin accumulation. *Infect. Immun.* 55:2681-2688.

Coleman, R. 1987. Bile salts and biliary lipids. *Biochem. Soc. Trans.* 15: 68S-80S.

Crawford, J. M., C. A. Berken, and J. L. Gollan. 1988. Role of the hepatocyte microtubular system in the excretion of bile salts and biliary lipid: implications for intracellular vesicular transport. *J. Lipid Res.* 29:144-156.

Donaldson, J. G., R. A. Kahn, J. Lippincott-Schwartz, and R. D. Klausner. 1991. Binding of ARF and β-COP to Golgi membranes: possible regulation by trimeric G protein. *Science (Wash. DC).* 254:1197-1199.

Drust, D. S., and C. E. Creutz. 1988. Aggregation of chromaffin granules by calpactin at micromolar levels of calcium. *Nature (Lond.).* 331:88-91.

Emans, N., J.-P. Gorvel, C. Walter, V. Gerke, R. Kellner, G. Griffiths, and J. Gruenberg. 1993. Annexin II is a major component of fusogenic endosomal vesicles. *J. Cell Biol.* 120:1357-1369.

Frimmer, M., and K. Ziegler. 1988. The transport of bile acids in liver cells. *Biochim. Biophys. Acta.* 947:75-99.

Gautam, A., O. C. Ng, and J. L. Boyer. 1987. Isolated rat hepatocyte couplets in short-term culture: structural characteristics and plasma membrane reorganisation. *Hepatology.* 7:216-223.

Gerke, V. 1991. p11, A member of the S-100 protein family, is associated with the tyrosine kinase substrate p36 (annexin II). *In* Novel Calcium Binding Proteins. Fundamentals and Clinical Implications. C. W. Heizmann, editor. Springer-Verlag, Berlin. pp. 139-155.

Groothius, G., M. J. Hardonk, K. P. T. Keulemans, P. Miervenhuis, and D. K. F. Meijer. 1982. Autoradiographic and kinetic demonstration of aci-

nar heterogeneity of taurocholate transport. *Am. J. Physiol.* 243:G455-G462.

Handel, S. E., M. E. Rennison, C. J. Wilde, and R. D. Burgoyne. 1991. Annexin II (calpactin I) in the mouse mammary gland: immunolocalization by light- and electron microscopy. *Cell Tissue Res.* 264:549-554.

Harder, T., and V. Gerke. 1993. The subcellular distribution of early endosomes is affected by the annexin II$_2$p11$_2$ complex. *J. Cell Biol.* 123:1119-1132.

Haussinger, D. 1990. Nitrogen metabolism in liver: structural and functional organization and physiological relevence. *Biochem. J.* 267:281-290.

Hayakawa, T., O. C. Ng, A. Ma, and J. L. Boyer. 1990. Taurocholate stimulates transcytotic vesicular pathways labeled by horse radish peroxidase in the isolated perfused rat liver. *Gastoenterology.* 99:216-228.

Helms, J. B., and J. E. Rothman. 1992. Inhibition by Brefeldin A of a Golgi membrane enzyme that catalyses exchange of guanine nucleotide bound to ARF. *Nature (Lond.).* 360:352-354.

Hubbard, A. L. 1991. Targeting of membrane and secretory proteins to the apical domain in epithelial cells. *Semin. Cell Biol.* 2:365-374.

Hugentobler, G., and P. J. Meier. 1986. Multispecific anion exchange in basolateral (sinusoidal) rat liver plasma membrane vesicles. *Am. J. Physiol.* 251:G656-G664.

Hunziker, W., J. A. Whitney, and I. Mellman. 1991. Selective inhibition of transcytosis by Brefeldin A in MDCK cells. *Cell.* 67:617-627.

Jungermann, K., and N. Katz. 1989. Functional specialisation of different hepatocyte populations. *Phys. Rev.* 69:708-763.

Kaplan, K. B., J. R. Swedlow, H. E. Varmus, and D. O. Morgan. 1992. Localization of pp60c-src with endosomal membranes in mammalian fibroblasts. *J. Cell Biol.* 118:321-334.

Kast, C., B. Stieger, K. H. Winterhalter, and P. J. Meier. 1994. Hepatocellular transport of bile acids. *J. Biol. Chem.* 269:5179-5186.

Knutton, S. K., T. Baldwin, P. H. Williams, and S. A. McNeish. 1989. Actin accumulation at sites of bacterial adhesion to tissue culture cells: basis of a new diagnostic test for enteropathogenic and enterohemorrhagic *Escherichia coli. Infect. Immun.* 57:1290-1298.

Lake, J. R., V. Licko, R. W. Van Dyke, and B. F. Scharschmidt. 1985. Biliary secretion of fluid-phase markers by the isolated perfused liver: role of transcellular vesicular transport. *J. Clin. Invest.* 76:676-684.

Lowe, P. J., K. S. Kan, S. G. Barnwell, R. Sharma, and R. Coleman. 1985. Transcytosis and paracellular movements of horseradish peroxide across liver parenchymal tissue from blood to bile. *Biochem. J.* 229:529-537.

Meier, P. J. 1989. The bile salt secretory polarity of hepatocytes. *J. Hepatology.* 9:124-129.

Mills, C. O., K. Rahman, R. Coleman, and E. Elias. 1991. Cholyl-lysyl fluorescein synthesis, biliary excretion in vivo and during single pass perfusion in isolated rat liver. *Biochem. Biophys. Acta.* 1115:151-156.

Moldeus, P., J. Hogberg, and S. Orrenius. 1978. Isolation and use of liver cells. *Methods Enzymol.* 52:60-71.

Muller, M., T. Ishikawa, U. Berger, C. Kluneman, L. Lucka, A. Schreyer, C. Kannicht, W. Reutter, G. Kurz, and D. Keppler. 1991. ATP-dependent transport of taurocholate across the hepatocyte canalicular membrane mediated by a 110 kDa glycoprotein binding ATP and bile salt. *J. Biol. Chem.* 266:18920-18926.

Nishida, T., Z. Gatmaitan, M. Che, and I. M. Arias. 1991. Rat liver canalicular membrane vesicles contain an ATP-dependent bile acid transport system. *Proc. Natl. Acad. Sci. USA.* 88:6590-6594.

Phillips, M. J., C. Oshio, M. Miyairi, H. Katz, and C. R. Smith. 1982. A study of bile canalicular contractions in isolated hepatocytes. *Hepatology.* 2: 763-768.

Ruetz, S., G. Fricker, G. Hugentobler, K. Winterhalter, G. Kurz, and P. J. Meier. 1987. Isolation and characterization of the putative canalicular bile salt transport system of rat liver. *J. Biol. Chem.* 262:11324-11330.

Sakisaka, S., O. C. Ng, and J. L. Boyer. 1988. Tubulovesicular transcytotic pathway in isolated rat hepatocyte couplets in culture: effect of colchicine and taurocholate. *Gastroenterology.* 95:793-804.

Sarafian, T., L. A. Pradel, J. P. Henry, D. Aunis, and M. F. Bader. 1991. The participation of annexin II (calpactin I) in cell-evoked exocytosis requires protein kinase C. *J. Cell Biol.* 114:1135-1147.

Stieger, B., B. O'Neill, and P. Meier. 1992. ATP-dependent bile salt transport in canalicular rat liver plasma-membrane vesicles. *Biochem. J.* 284:67-74.

Stolz, A., H. Takikawa, M. Ookhtens, and N. Kaplowitz. 1989. The role of cytoplasmic proteins in hepatic bile acid transport. *Annu. Rev. Physiol.* 51:161-176.

Weinman, S. A., J. Graf, and J. L. Boyer. 1989. Voltage-driven, taurocholate dependent secretion in isolated rat hepatocyte couplets. *Am. J. Physiol.* 256:G826-G832.

Weinman, S. A., and R. P. Weeks. 1993. Electrogenicity of Na-coupled bile salt transport in isolated rat hepatocytes. *Am. J. Physiol.* 265:G73-G78.

Wilton, J. C., J. K. Chipman, C. J. Lawson, A. J. Strain, and R. Coleman. 1993a. Periportal- and perivenous-enriched hepatocyte couplets: differences in canalicular activity and in response to oxidative stress. *Biochem. J.* 292:773-779.

Wilton, J., R. Coleman, D. L. Lankaster, and J. K. Chipman. 1993b. Stability and optimisation of canalicular function in hepatocyte couplets. *Cell Biochem. Function.* 11:179-186.

Zimmerli, B., J. Valantinas, and P. J. Meier. 1989. Multispecificity of Na$^+$-dependent taurocholate uptake in basolateral (sinusoidal) rat liver plasma membrane vesicles. *J. Pharmacol. Exp. Ther.* 250:301-308.